ISSN 1063-7745, Crystallography Reports, 2009, Vol. 54, No. 2, pp. 306–312. © Pleiades Publishing, Inc., 2009.
Original Russian Text © N.M. Demyanyshyn, B.G. Mytsyk, A.S. Andrushchak, O.V. Yurkevych, 2009, published in Kristallografiya, 2009, Vol. 54, No. 2, pp. 331–337.

PHYSICAL PROPERTIES OF CRYSTALS

Anisotropy of the Electro-Optic Effect in Magnesium-Doped $LiNbO_3$ Crystals

N. M. Demyanyshyn, B. G. Mytsyk, A. S. Andrushchak, and O. V. Yurkevych

Institute of Physics and Mechanics, Lviv, Ukraine

e-mail: mytsyk@ipm.lviv.ua

Received June 2, 2008

Abstract—Specific features of constructing indicatory surfaces of the electro-optic effect (EOE) are described. The generalized case for the symmetry class 3*m* and all three possible indicatory surfaces under orthogonal experimental conditions, when the directions of light propagation and electric field are orthogonal, is considered. The EOE surfaces are constructed for magnesium-doped lithium niobate crystals. The specific features of anisotropy of these surfaces are discussed and their extreme values and corresponding angular coordinates are found. To construct the indicatory surfaces, all absolute coefficients of the linear electro-optic effect are determined by the interferometric method. The difference in the electro-optic coefficients of pure and magnesium-doped crystals does not exceed 10%. An advantage of doped crystals is their high durability to high-power laser radiation.

PACS numbers: 77.84.Dy; 78.20.Jq

DOI: 10.1134/S1063774509020217

INTRODUCTION

The basic data on the indicatory surfaces of physical effects, which most completely reflect their anisotropy, are considered in detail in classical textbooks of crystal physics [1–3]. The specific results of the study of the anisotropy of piezoelectric, elastic, and piezoresistive effects by constructing indicatory surfaces were reported in [4–7], and the specific features of construction of indicatory surfaces of photoelastic effects were considered in [8–11].

In this study, electro-optic indicatory surfaces were constructed for magnesium-doped (7% MgO in a melt) $LiNbO_3$ crystals. Construction of such surfaces and their analysis is the shortest way for determining the orientation of samples and geometries of their application in design of electro-optic modulators based on new electro-optic materials.

GENERAL EXPRESSION FOR ELECTRO-OPTIC INDICATORY SURFACES IN SPHERICAL COORDINATES

We will proceed from the tensor form of the equation for indicatory surfaces of the electro-optic effect (EOE), which corresponds to the transformation for the third-rank tensor component at rotation of the coordinate system [3]:

$$r'_{unh} = \alpha_{up}\alpha_{nc}\alpha_{hl}r_{pcl}, \quad (1)$$

where α_{up}, α_{nc}, and α_{hl} are the direction cosines of the radius vector **r**, describing the indicatory surface r'_{unh} in the crystal-physical coordinate system X_1, X_2, X_3, and r_{pcl} are the electro-optic tensor components.

Llithium niobate crystals belong to the high-symmetry class 3*m* and have only four independent electro-optic coefficients: r_{22}, r_{13}, r_{33}, and r_{51}. Therefore, (1) in matrix notation has a simple form:

$$\begin{aligned} r'_{ie} = {} & [\alpha_{e2}(\alpha_{i2}^2 - \alpha_{i1}^2) - 2\alpha_{i1}\alpha_{i2}\alpha_{e1}]r_{22} \\ & + (\alpha_{i1}^2\alpha_{e3} + \alpha_{i2}^2\alpha_{e3})r_{13} + \alpha_{i3}^2\alpha_{e3}r_{33} \\ & + 2\alpha_{i3}(\alpha_{i1}\alpha_{e1} + \alpha_{i2}\alpha_{e2})r_{51}. \end{aligned} \quad (2)$$

To construct the EOE surfaces, formula (2) should be written in spherical coordinates. To this end, we will write the direction cosines of the electric field vector **E** and the vector **i** of light wave oscillations in the spherical coordinate system. Let these vectors **E** be related to the crystallophysical axes X_1, X_2, and X_3 through angles β and α (vector **i**) and θ and φ (vector **i**) (Fig. 1).

Then, the direction cosines of the vector **E** can be written as

$$\alpha_{e1} = \sin\beta\cos\alpha, \quad \alpha_{e2} = \sin\beta\sin\alpha, \quad \alpha_{e3} = \cos\beta, \quad (3)$$

where β is the angle between the vector **E** and the X_3 axis and α is the angle between the projection of **E** onto the X_1OX_2 plane and the X_1 axis.

Similarly, the direction cosines of vector **i** have the form

$$\alpha_{i1} = \sin\theta\cos\varphi, \quad \alpha_{i2} = \sin\theta\sin\varphi, \quad \alpha_{i3} = \cos\theta, \quad (4)$$

where θ is the angle between the vector **i** and the X_3 axis and φ is the angle made by the projection of **i** onto the X_1OX_2 plane with the X_1 axis (Fig. 1).

Substituting expressions (3) and (4) into (2), we obtain the general equation of the surface of linear EOE for crystals of the 3*m* symmetry class in the spherical coordinate system:

$$r'_{ie} = r(\beta, \alpha, \theta, \varphi)$$
$$= [r_{13}\cos\beta - r_{22}\sin\beta\sin(\alpha + 2\varphi)]\sin^2\theta \quad (5)$$
$$+ r_{33}\cos\beta\cos^2\theta + r_{51}\sin\beta\cos(\alpha - \varphi)\sin 2\theta,$$

where r'_{ie} is the length of the radius vector **r**, i.e., the EOE value in an arbitrary direction **i**, set by the angles θ and φ, under electric field **E** applied in an arbitrary direction, set by the angles β and α.

To construct specific EOE surfaces in magnesium-doped lithium niobate crystals ($LiNbO_3$:MgO) on the basis of (5), we used the following values of the linear EOE coefficients r_{ie} (in 10^{-12} m/V): $r_{22} = 7.47 \pm 0.21$, $r_{13} = 10.9 \pm 0.3$, $r_{33} = 34.3 \pm 0.8$, and $r_{51} = 34.9 \pm 1.3$ (they were obtained by us according to the technique [12]).

Figure 2 shows the examples of EOE surfaces $r'_{ie} = r(\theta, \varphi)$, describing the change in the refractive index in space under an electric field applied in specific directions (β, α). The main cross sections of these surfaces by the X_2OX_3; X_1OX_3, and X_1OX_2 planes correspond to zero coordinates of the $x_1 = 0$, $x_2 = 0$, and $x_3 = 0$ surfaces, respectively, or, in the spherical coordinate system (Fig. 1), to the angles $\varphi = 90°$, $\varphi = 0°$, and $\theta = 90°$, respectively. For example, we obtain a circular cross section of the indicatory surface in Fig. 2a by substituting $\beta = \alpha = 0$ into (5),

$$r(\theta, \varphi) = r_{13}\sin^2\theta + r_{33}\cos^2\theta, \quad (6)$$

and then substituting $\theta = 90°$ (which corresponds to $x_3 = 0$) into (6),

$$r(90°, \varphi) = r_{13} \quad (\text{for all } \varphi). \quad (7)$$

Expression (7) gives a circle with a radius r_{13}.

EXAMPLES OF ANALYSIS OF EOE SURFACES

(i) Figure 2a (construction for the case $\beta = \alpha = 0°$) shows that the maximum value of the radius vector of this surface corresponds to the direction of the X_3 axis (when θ and φ are zero). In this case, $r'(\theta, \varphi) = r_{33} = 34.3 \times 10^{-12}$ m/V. Substituting zeros instead of θ, φ, β, and α into (5) or $\theta = \varphi = 0°$ into (6), we make sure that $r'(\theta, \varphi) = r_{33}$.

(ii) Except for the case in Fig. 2a, the directions of the largest change in the refractive index do not coincide with the directions of crystallophysical axes. This is demonstrated in Figs. 2b–2d. For example, in Fig. 2c,

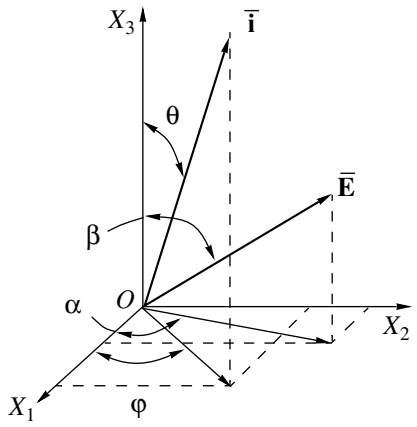

Fig. 1. Spherical coordinates of unit vectors **i**(θ, φ) and **E**(β, α).

the maximum EOE value approximately corresponds to the diagonal direction between the X_2 and X_3 axes. Analysis of this surface with study of function (5) for extreme values (using standard software) revealed the maximum effect value in this crystal to be $r'(\theta, \varphi) = 44.8 \times 10^{-12}$ m/V at the angular coordinates $\beta = 55°$ and $\alpha = 90°$ for the electric field vector **E** and $\theta = 41°$ and $\varphi = 90°$ for the vector **i** of light wave oscillations. These conditions of extreme EOE value are difficult to realize in practice, because the vectors **i** and **E** are not orthogonal.

(iii) The EOE in $LiNbO_3$:MgO crystals has a significant anisotropy, including the change in the sign of the effect. Figures 2b–2d show the positive and negative lobes of the surfaces. Therefore, the surfaces $r'_{ie} = r'(\beta, \alpha, \theta, \varphi)$ have zero values in certain directions. For example, when **E** has the direction $\beta = 90°$, $\alpha = 0°$ (Fig. 2b), zero EOE values are in the X_2OX_3 plane, i.e., at $\varphi = 90°$ and any θ. One can make sure of this algebraically, substituting $\beta = 90°$, $\alpha = 0°$, and $\varphi = 90°$ into (5).

Let us consider a more complex case: the vector **E** has the direction $\beta = 90°$, $\alpha = 90°$ (Fig. 2d), the directions of zero values $r'(\theta, \varphi)$ are determined by equating relation (5) or the equation of the corresponding cross section to zero. For example, the cross section of surface (5) by the X_2OX_3 plane ($\varphi = 90°$) has the form (with allowance for previously formulated condition $\beta = \alpha = 90°$)

$$r(\theta, \varphi) = r_{22}\sin^2\theta + r_{51}\sin 2\theta. \quad (8)$$

To determine the angles θ corresponding to zero EOE in the cross section (8), we equate the right-hand side of Eq. (8) to zero with factorization of the general factor $\sin\theta$:

$$\sin\theta(r_{22}\sin\theta + 2r_{51}\cos\theta) = 0. \quad (9)$$

As a result, we have two solutions: $\theta_1 = 0$ and $\theta_2 = \arctan(-2r_{51}/r_{22}) = \arctan(-9.34) = -83.9°$. The first

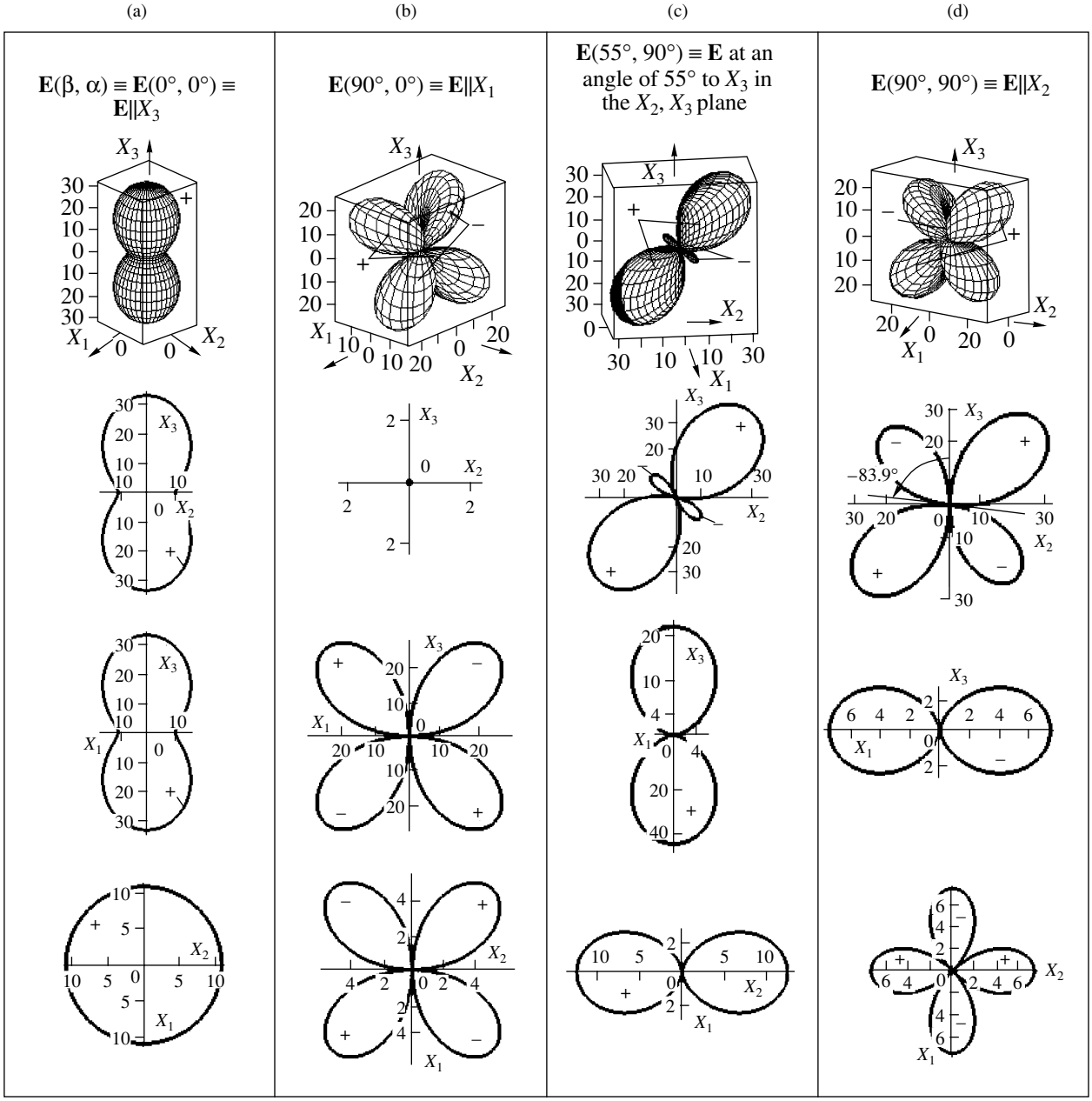

Fig. 2. EOE surfaces $r'(\theta, \varphi)$ under **E** in different directions (β, α) and their cross sections by main planes (in units 10^{-12} m/V) for $LiNbO_3$:MgO crystals.

solution corresponds to the X_3 axis and the other one is shown by a straight line in Fig. 2d (cut X_2, X_3). The negative angle θ_2 is counted to the left from the X_3 axis (Fig. 1).

(iv) The EOE surfaces for pure lithium niobate crystals are similar to those for $LiNbO_3$:MgO (Fig. 2), because the EOE coefficients for pure crystals ($r_{22} = 6.79 \pm 0.04$, $r_{13} = 10.1 \pm 0.5$, $r_{33} = 33.2 \pm 1.3$, and $r_{51} = 32.1 \pm 1.5$ (in 10^{-12} m/V)) [12] do not significantly differ from those for doped crystals. The directions of EOE extrema in pure and doped crystals coincide, while the maximum effect values in doped crystals are somewhat larger (to 10%), in correspondence with the larger electro-optic coefficients r_{ie}.

(v) Note that items (i)–(iv) give examples of analysis of the $r'(\theta, \varphi)$ surfaces at fixed directions of the electric field $\mathbf{E}(\beta, \alpha)$, i.e., these surfaces describe the radius vector **r** coinciding with the vector **i** of light wave oscillations, whose value corresponds to the change in the refractive index n_i. Obviously, construction can be performed in another way: the direction $\mathbf{i}(\theta, \varphi)$ is fixed, and the surface is described by the radius vector **r**, coin-

ciding with the electric field vector **E**. In this way, we obtain the surfaces $r'(\beta, \alpha)$ at different directions of **i**(θ, φ). The corresponding surfaces describe the change in the refractive index n_i in a fixed direction, specified by the angles θ and φ at a change in **E** in the entire space. For example, substituting $\theta = 0°$ into (5) (then **i** $\parallel X_3$), we obtain the expression describing the change in n_i along X_3 at all values of β and α:

$$r'(\beta, \alpha) = r_{33}\cos\beta. \quad (10)$$

Surface (10) is formed by two spheres with a diameter r_{33}: a positive sphere above the X_1OX_2 plane and a negative sphere below this plane.

There is a more complex case: $\theta = 45°$ and $\varphi = 90°$. The corresponding surface describes the change in the refractive index in the diagonal direction between the X_2 and X_3 axes under electric field **E** in all (β, α) directions. Substituting the noted values θ and φ into (5), we obtain

$$r'(\beta, \alpha) = \frac{1}{2}(r_{13} + r_{33})\cos\beta + \left(\frac{1}{2}r_{22} + r_{51}\right)\sin\beta\sin\alpha. \quad (11)$$

This is a complex surface with positive and negative parts. Let us investigate it on extrema. The derivative with respect to β can be written as

$$\partial r/\partial\beta = -\frac{1}{2}(r_{13} + r_{33})\sin\beta + \left(\frac{1}{2}r_{22} + r_{51}\right)\cos\beta\sin\alpha. \quad (12)$$

It follows from (11) that, since all coefficients r_{ie} are positive, the effect will be maximum at the maximum of $\sin\alpha$ (when $\alpha = 90°$), i.e., in the X_3OX_2 plane. Substituting this value of α into (12) and equating the right-hand side of (12) to zero, we obtain

$$\tan\beta = (r_{22} + 2r_{51})/(r_{13} + r_{33}) = 1.71. \quad (13)$$

From expression (13), we find $\beta = \arctan 1.71 = 59.7°$. Using this value of β and taking into account that $\alpha = 90°$, we derive the EOE maximum from (11): $r'_{\max}(\beta, \alpha) = r'_{\max}(59.7°, 90°) = 44.76 \times 10^{-12}$ m/V. This maximum is somewhat smaller than the EOE maximum in $LiNbO_3$:MgO crystals (see (ii)). Similarly, one can find $r'_{\max}$ and the corresponding angles β for other planes passing along the X_3 axis. To this end, it is necessary to substitute the specific values of α into (11) and (12). For example, at $\alpha = 30°$, we have $r'_{\max}(40.5°, 30°) = 29.8 \times 10^{-12}$ m/V, etc.

(vi) Obviously, there are many interesting surfaces $r'(\theta, \varphi)$ at fixed β and α and surfaces $r'(\beta, \alpha)$ at fixed θ and φ. However, we restrict ourselves to the analysis in (i)–(v), because the extreme values of the radius vectors of these surfaces generally do not correspond to the orthogonal directions of light propagation and electric field; i.e., **k** and **E** are not orthogonal (**k** is the vector describing the light propagation). Below, we consider the electro-optic indicatory surfaces constructed for orthogonal vectors **k** and **E**. Such surfaces are interesting in design of electro-optic light modulators.

EOE INDICATORY SURFACES FOR ORTHOGONAL GEOMETRIES OF THE EXPERIMENT

Such experimental conditions imply that the electric field **E** and light propagation direction **k** are orthogonal (for the photoelastic effect, such surfaces were considered in detail in [8, 9, 13–15]). Then, only three different EOE surfaces are possible. Let us consider them.

(i) The indicatory surface of a longitudinal EOE, when the refractive index n_i is measured in the same direction **i** in which the electric field **E** acts, i.e., (**r** $\parallel$ **i** $\parallel$ **E**). This condition corresponds to the case $\beta = \theta$ and $\alpha = \varphi$ (Fig. 1). Substituting these equalities into (5), we obtain the expression describing the longitudinal EOE surface:

$$r'_{ii}(\theta, \varphi) = -r_{22}\sin^3\theta\sin 3\varphi + (r_{13} + 2r_{51})\sin^2\theta\cos\theta + r_{33}\cos^3\theta. \quad (14)$$

(ii) Transverse EOE, where **i** $\perp$ **E**, allows two versions of indicatory surfaces. The surface is described by the radius vector **r** coinciding with **i** (**r** $\parallel$ **i**), while **E** $\perp$ **i** changes its direction in the X_1OX_2 plane. These conditions, according to Fig. 1, are satisfied at $\beta = 90°$ and $\alpha = \varphi + 90°$. Substituting these dependences into (5), we obtain the equation of transverse EOE:

$$r'^{(i)}(\theta, \varphi) = -r_{22}\sin^2\theta\cos 3\varphi. \quad (15)$$

We will refer to surface (15) as the polarization indicatory surface, because it is described by the radius vector **r** coinciding with the vector **i** of light wave (polarization) oscillations.

(iii) Another version of the transverse EOE surface is described by the radius vector **r** coinciding with the electric field direction **E** (**r** $\parallel$ **E**), while **i** changes its direction in the X_1OX_2 plane. Then, according to Fig. 1, we have the following relation between the spherical coordinates: $\theta = 90°$ and $\varphi = \alpha + 90°$. Substitution of these conditions into (5) yields another equation of transverse EOE:

$$r'^{(E)}(\beta, \alpha) = r_{22}\sin\beta\sin 3\alpha + r_{13}\cos\beta. \quad (16)$$

We refer to surface (16) as the electric field indicatory surface, because it is described by the radius vector **r** coinciding with the electric field vector **E**.

Surfaces (14)–(16) and their cross sections by the main planes are shown in Fig. 3.

EXAMPLES OF ANALYSIS OF EOE SURFACES FOR ORTHOGONAL EXPERIMENTAL CONDITIONS

(i) Figure 3 shows that the maximum EOE value corresponds to the surface $r'_{ii}(\theta, \varphi)$ of longitudinal EOE. In this case, the directions of the radius vectors with the largest effect value ($r'_{ii} = 43 \times 10^{-12}$ m/V) do not coincide with any of the principal axes (X_1, X_2, X_3).

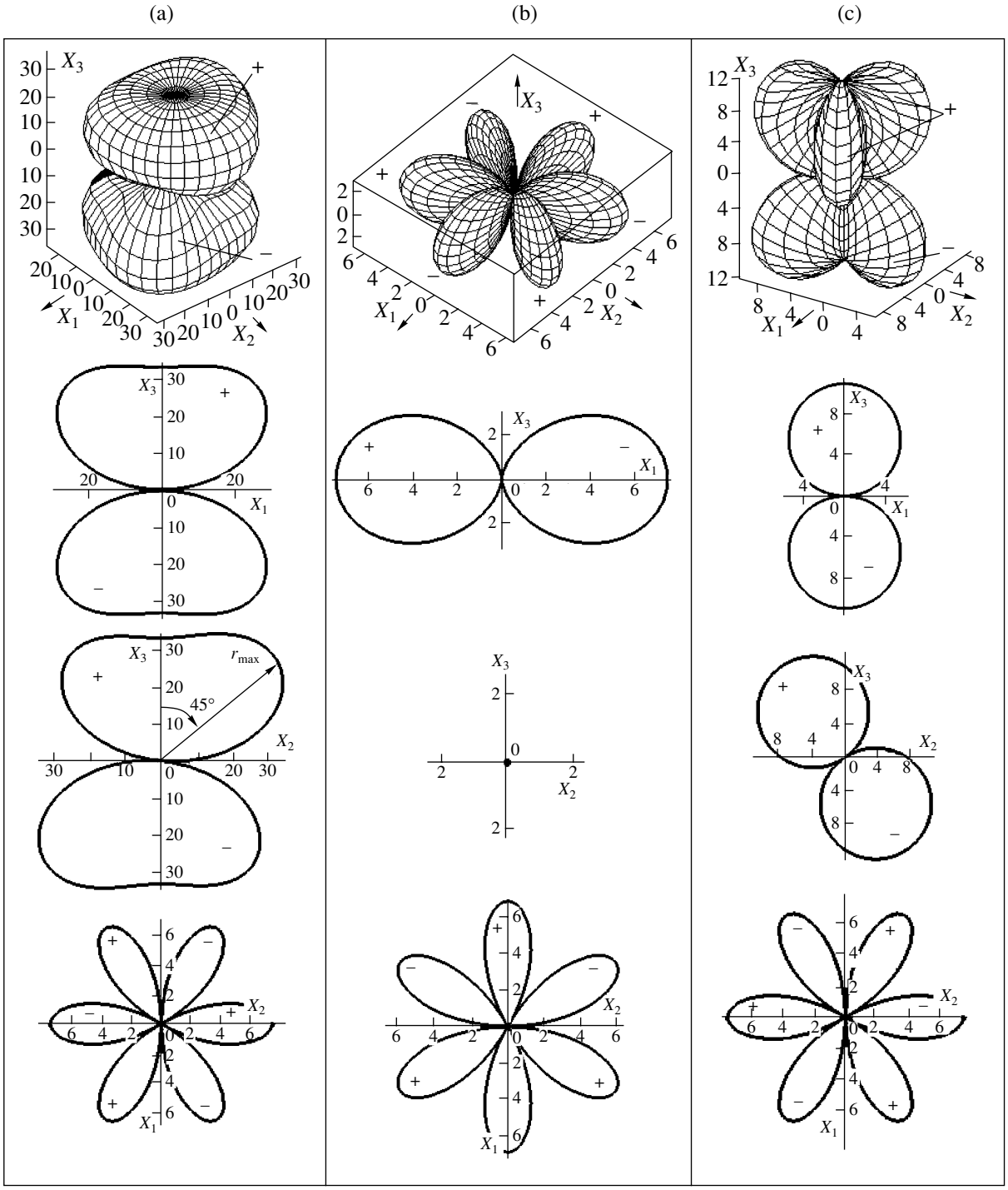

Fig. 3. EOE indicatory surfaces in $LiNbO_3$:MgO crystals under orthogonal experimental conditions and their main cross sections: (a) longitudinal r'_{ii}, (b) transverse $r'^{(i)}$, and (c) $r'^{(E)}$.

For example, one of the maxima occurs at the angular coordinates $\theta = 45°$ and $\varphi = 90°$ and is, respectively, in the X_2OX_3 plane. The direction of this maximum is denoted by a straight line in the X_2, X_3 cross section (Fig. 3a). Such maxima are repeated with a period of 120° for two more angles φ, whose values are listed in the table. The values of these maxima and their angular coordinates are determined using the standard software. Note that this value of the longitudinal EOE maxima under orthogonal experimental conditions exceeds

by 25% the electro-optic coefficient $r_{33} = 34.3 \times 10^{-12}$ m/V, which corresponds to the longitudinal EOE value along the optical X_3 axis. Note that this maximum longitudinal EOE value $r'_{ii}(\theta, \varphi)$ is on the same order of magnitude as the maximum possible effect value in this crystal: 44.8×10^{-12} m/V (see (ii) in analysis of the surfaces shown in Fig. 2).

(ii) Zero longitudinal EOE values $r'_{ii}(\theta, \varphi)$ are observed for all φ; in this case, each φ value has a corresponding θ value, and these θ values may vary from 85° to 95° (or ±5° with respect to the X_1OX_2 plane). Three angles θ (separated by rotation by 120°), $\varphi = 30°$, 150°, and 270° for $\theta = 85°$ and $\varphi = 90°$, 210°, and 330° for $\theta = 95°$, correspond to the extreme values of the noted range of $r'_{ii}(\theta, \varphi) = 0$. Obviously, the reproducibility of the values $r'_{ii}(\theta, \varphi) = 0 = 0$ with a period of 120° and reproducibility of the $r'_{ii}(\theta, \varphi)$ peaks with the same period (see (i)) correspond to a threefold symmetry axis, which coincides with the X_3 axis for the $3m$ class.

Zero values of the transverse EOE indicatory surface $r'^{(E)}(\beta, \alpha)$ are arranged similarly; however, β changes in the angular range from 124° (at $\alpha = 30°$) to 56° (at $\alpha = 90°$), etc. Concerning the polarization indicatory surface $r'^{(i)}(\theta, \varphi)$, its zero values lie in the planes passing through the X_3 axis for all θ at $\varphi = 30° + N \times 60°$, where $N = 0, 1, 2, \ldots, 5$. Note that $\varphi = 90°$ at $N = 1$, a situation corresponding to the cross section of the surface $r^{(i)}(\theta, \varphi)$ by the main plane X_1OX_3. This "zero" cross section is shown in Fig. 3b.

(iii) Other interesting specific features of the cross sections of the surfaces shown in Fig. 3 are as follows: (1) for the longitudinal EOE, the change in θ in a wide range corresponds to a large EOE value (Fig. 3a, cross sections X_1, X_3 and X_2, X_3); this property reduces the requirements for strict orientation of the samples in engineering calculations; (2) the X_1 and X_2 cross sections of all three indicatory surfaces are identical in shape and value; (3) the cross sections of the surface $r'^{(E)}(\beta, \alpha)$ by the main planes X_1OX_3 and X_2OX_3 are circular (Fig. 3c); and the formula for these cross sections can easily be obtained by substituting $\alpha = 0°$ and $\beta = 90°$, respectively, into (16).

(iv) As in the case of general EOE surfaces (Fig. 2), the surfaces under orthogonal experimental conditions (Fig. 3) for pure and magnesium-doped lithium niobate crystals are almost identical because the absolute coefficients r_{ie} are almost identical for these crystals. The maximum values of the radius vectors of these surfaces and their angular (spherical) coordinates are also close (table).

Hence, we can conclude that doping of lithium niobate crystals with magnesium oxide (7% MgO in the melt) does not lead to a significant change in the EOE value and spatial anisotropy. An advantage of doped crystals is that they have a higher (by a factor of 5) optical beam durability [16]. Thus, $LiNbO_3$:MgO is a promising material for electro-optic control of high-power laser radiation.

Maximum values of the linear EOE indicatory surface (in 10^{-12} m/V) for magnesium-doped and pure (denoted by asterisks) $LiNbO_3$ crystal at $T_K = 20°C$; $\lambda = 0.63$ μm

Indicatory surfaces	Maximum values			
	value of electro-optic effect		θ, deg	φ, deg
r'_{ii}	±43.4	±40.4*	45 135	90, 210, 330 30, 150, 270
$r'^{(i)}$	±7.5	±6.79*	90	0, 60, 120, 180, 240, 300
$r'^{(E)}$	±13	±12*	34 (31*) 145 (149*)	30, 150, 270, 90, 210, 330

CONCLUSIONS

In [8, 9], the equations of piezo-optic surfaces were obtained in the general form by determining the difference in the radius vectors of the perturbed and free optical indicatrices ($r_v - r$). In this study, such an equation for EOE is derived in a simpler way. Specifically, the expressions for the direction cosines of the radius vectors in spherical coordinates are written and substituted into the general equation (2) simultaneously for the light wave polarization vector **i** and electric field vector **E**. The total equation (5) is checked also by determining the difference in the radius vectors of the indicatrix $r_v - r$. Thus, it is shown for EOE that the difference $r_v - r$ is identical to the law of transformation of the EOE tensor components under rotation of the coordinate system. Proof of this statement is omitted because these questions were considered in detail in [8, 9] for the piezo-optic effect.

Examples of some EOE surfaces for lithium niobate crystals doped with magnesium oxide are shown and the specific features of spatial anisotropy of the effect are discussed. It is shown that the EOE value and anisotropy in pure and doped crystals are almost identical. An advantage of the latter is that their optical beam durability is higher by a factor of about 5; hence, they are promising for application in electro-optic modulators of high-power laser radiation.

ACKNOWLEDGMENTS

We are grateful to I.M. Sol'skiĭ for supplying $LiNbO_3$:MgO crystal samples.

REFERENCES

1. J. F. Nye, *Physical Properties of Crystals* (Oxford Univ. Press, London, 1964; Mir, Moscow, 1967).
2. Yu. I. Sirotin and M. P. Shaskol'skaya, *Fundamentals of Crystallography* (Nauka, Moscow, 1979) [in Russian].
3. *Modern Crystallography*, Vol. 4: *Physical Properties of Crystals*, Ed. by L. A. Shuvalov, A. A. Urusovskaya, I. S. Zheludev, et al. (Nauka, Moscow, 1981) [in Russian].
4. Sh. M. Butabaev and I. I. Smyslov, Kristallografiya **16** (4), 796 (1971) [Sov. Phys. Crystallogr. **16**, 688 (1971)].
5. Sh. M. Butabaev, N. V. Perelomova, and I. I. Smyslov, Kristallografiya **17** (3), 678 (1972) [Sov. Phys. Crystallogr. **17**, 593 (1972)].
6. Sh. M. Butabaev and Yu. I. Sirotin, Kristallografiya **18** (1), 195 (1973) [Sov. Phys. Crystallogr. **18**, 121 (1973)].
7. H. Pengdi, Ya. Weiling, T. Jian, et al., Appl. Phys. Lett., **86**, 052 902 (2005).
8. B. G. Mytsyk and N. M. Dem'yanishin, Kristallografiya **51** (4), 696 (2006) [Crystallogr. Rep. **51**, 653 (2006)].
9. N. M. Dem'yanishin, B. G. Mytsyk, and B. M. Kalynyak, Ukr. Fiz. Zh. **50**, 521 (2005).
10. M. V. Kaidan, A. S. Andrushchak, M. N. Klymash, et al., Ukr. J. Phys. **48**, 1104 (2003).
11. B. Mytsyk, Ukr. J. Phys. Optics **4**, 105 (2003).
12. A. S. Andrushchak, B. G. Mytsyk, N. M. Dem'yanishin, et al., Vestn. NU Lvivska Politekhnika, Ser. Electron., No. 592, 148 (2007).
13. A. S. Andrushchak, B. G. Mytsyk, and O. V. Lyubich, Ukr. Fiz. Zh. **37**, 1217 (1992).
14. B. G. Mytsyk, A. S. Andrushchak, N. M. Dem'yanishin, and L. M. Yakovleva, Kristallografiya **41** (3), 500 (1996) [Crystallogr. Rep. **41**, 472 (1996)].
15. M. V. Kaidan, B. V. Tybinka, A. V. Zadorozhna, et al., Opt. Mater. **29**, 475 (2007).
16. D. Yu. Sugak, A. O. Matkovskii, I. M. Solskii, et al., Cryst. Res. Technol **32**, 805 (1997).

Translated by A. Sin'kov